
Carbon
2008
Carbon
2008
CARBON'08
International Conference on Carbon
World Conference on Carbon
13th (Sun.) - 18th (Fri.) July 2008
Chairman: Prof. M. Endo
E-mail: endo@endomoribu.shinshu-u.ac.jp
Editorial Manager: Prof. Y. Kaburagi
E-mail: ykabura@sc.musashi-tech.ac.jp
NAGANO, JAPAN

ESR OF ACTIVATED CARBON FIBERS WITH DIFFERENT SORBATES

Maxim A. Ziatdinov, Vladimir V. Kainara, Yuriy M. Nikolenko, Albert M. Ziatdinov
Institute of Chemistry, Far Eastern Branch of the Russian Academy of Sciences,
159, Prospect 100-letiya, 690022 Vladivostok,
Russia

Introduction

Activated carbons are representative porous materials, which have been widely used in various technologies (Marsh 2001). Activated carbon fibers (ACFs), which have large specific surface areas ranging about 1000-3000 m^2g^{-1}, are microporous carbons consisting of a three dimensional disordered network of micrographites, where each micrographite has three to four graphene sheets with an average in-plane size about a few nanometers (Marsh 2001, Kaneko *et al*. 1998) This particular structure makes ACFs a good model system of nanographites. There are a few reasons for an intently interest of scientists to nanographites. First, due to their intermediate position between the bulk graphite and aromatic molecules, nanographites are the potential source of new chemical substances with unusual electronic and magnetic properties. Second, while the fullerenes and carbon nanotubes are the close shaped pi-electron conjugated systems (Dresselhaus *et al*. 1996) the electronic properties of which are mainly controlled by the quantum size and surface effects, the nanographites represent the edge-open pi-electron conjugated system.

The presence of open edges around the peripheral region can result in occurrence of specific features in nanographite systems, which are different from their closed-surface counterparts (Fujita *et al.* 1996, Nakada *et al*. 1996). Obviously, an arbitrary shaped graphene sheet comprises two kinds of edges: zigzag type and armchair type, while the former has a *trans*-polyacetylene type structure, while the later has a *cis*-poliacetylene type. The calculations for the model of graphite ribbons – one dimensional graphite lattices of finite width, show that ribbons with zigzag edges possess edge states with energies close to the Fermi level (Fujita *et al.* 1996, Nakada *et al*. 1996). These edge states correspond to the nonbonding molecular orbital (nonbonding pi levels superimposed on the bonding pi and antibonding pi* bands). In contrast, edge states are completely absent for ribbons with armchair edges. However, in a general finite graphene sheet consisting of both types of edges, even a few zigzag sites per sequence are shown to lead to non-negligible edge-state effects, resulting in an enhancement in the electronic density of states around the Fermi energy (Nakada *et al*. 1996). The theoretical investigations of the stacking effects in the zigzag nanographite sheets show that the edge states are sensitive to the type of the graphene layers stacking and to the interlayer interaction (Narigaya 2001, Narigaya and Enoki 2002). At last, it was shown that the edge states might determine the new magnetic properties in nanographene sheet, because of their relatively large contribution to the density of states at the Fermi energy (Fujita *et al.* 1996). The calculations show a remarkable difference in the magnetic properties between the different types of graphene layers stacking (Narigaya 2001, Narigaya and Enoki 2002, Shyu and Lin 2003). Recently, the reality of edge states was proved experimentally (Niimi *at al*. 2005, Klusek *et al*. 2005, Kobayashi *et al*. 2005).

In this paper, we present the results of ESR, magnetic susceptibility, X-ray diffraction and X-ray photoelectron spectroscopy studies of nanographites – the structural elements (blocks) of ACFs, and their compounds with some substances.

Results and Discussion

The X-ray diffractograms of the ACFs show very broad peaks at the graphite (002), (100) and (101) positions, where graphite (100) and (101) peaks merge into a single broad peak around 20^0 (Fig. 1). In order to estimate the sizes of the graphite nanoparticles in ACFs, the intensities of the experimental X-ray diffractograms were corrected by standard procedures.

Using the corrected (002), (100) and (101) peak parameters we estimate the thickness and the in-plane size of the particle grains. From the broad graphite (002) peak, we find a grain thickness of $L_c \approx$1-1,2 nm. We deconvulate the broad feature around 20^0-24^0 into single (100) and (101) peaks on the assumption that each peak originates mostly from a single component. The obtained contribution to the

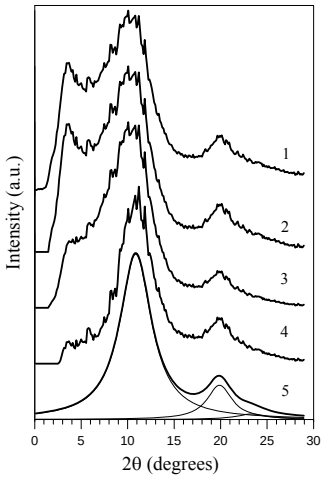

Figure 1. The X-ray diffraction spectra of ACFs. (1 – experimental; 2 – after constant background subtraction; 3 – after correction with Lorenz-polarization factor, carbon atomic form-factor and absorption factor; 4 – after angle dependant background subtraction; 5 – simulated spectrum with components, corresponding to (002), (100) and (101) peaks).

(100) peak gives an estimate of the in-plane size of $L_a \approx 2$ nm. From the location of centre for the (002) diffraction peak the interlayer distance between graphene sheets in evacuated samples are estimated at 0,4 nm, which are considerably longer than the interlayer distance of 0.3354 nm for bulk regular graphite. From nanographite sample thickness and interlayer distance between graphene sheets, the number of graphene sheets is estimated at ≈3-4.

The C1s spectrum of ACFs consists only of a single peak with the binding energy 284,4±0,1 eV. The lineshape parameters of signal considered are near the same for bulk graphite.

The ESR spectrum of ACFs reveals two Lorentzian signals (Fig. 2). At temperatures above ≈150 K only single signal from conduction electrons with a linewidth ≈6 mT is observed. Below ≈150 K, a second narrow signal from localized spins appears with a linewidth ≈0,1 mT. The *g*-values are estimated at *g*=2,0027(3) and 2,0033(3) for the signals from conduction electrons and localized states, respectively.

The magnetization curve shows the absence of the residual magnetization at different constant magnetic fields. The temperature dependence of the magnetic susceptibility χ_g for ACFs investigated is well described by the expression χ_g=1.318E-5/(*T*+0.9)-0.61E-6 (Fig. 3). From this low, it follows that approximately one localized spin per 2500 carbon atoms (or ~1 localized spin per ~10 nanographites) are presented in fibers at low temperatures.

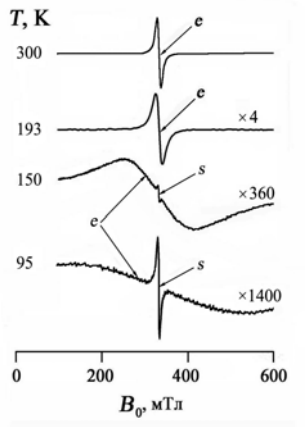

Figure 2. The ESR spectra of ACFs. (e – and s – the signals from conduction and localized electrons, respectively).

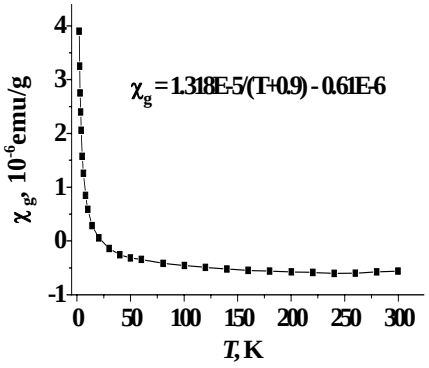

Figure 3. The magnetic susceptibility vs. temperature for the ACFs under a constant magnetic field of H_0 = 0.5 T.

From comparison of integral intensities of signals from conduction electrons and localized spins (the concentration of latter is known from the magnetic susceptibility data), the density of states near the Fermi level in nanographites was estimated. Such calculations show, that it is more than one order of magnitude larger than in bulk regular graphite at the same value of Fermi energy (Dresselhaus and Dresselhaus 1981). The results obtained unambiguously indicate the presence of an additional band around the Fermi energy in nanographites that was proposed theoretically (Fujita *et al.* 1996, Nakada *et al*. 1996). Another reason of considered phenomenon is the deeper position of Fermi level in

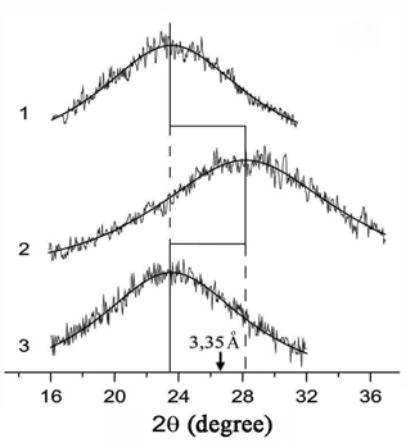

Figure 4. The changes of (002) X-ray diffraction peak for graphite nanoparticles – structural blocks of ACFs at absorption and desorption of water molecules. (1 – initial, 2 (3) – after adsorption (desorption) of water molecules).

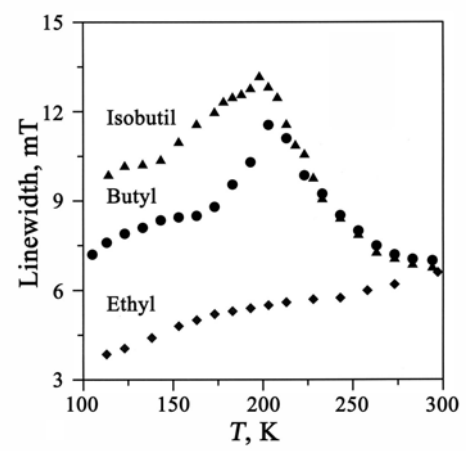

Figure 5. The CESR linewidth of ACFs with isobutyl, butyl and ethyl spirits vs. temperature.

Table 1. Displacement of the (002) X-ray diffraction peak in ACFs with spirits.

Spirit	Formula	Δ(2θ), degree
Methyl	CH_3OH	2,38
Ethyl	C_2H_5OH	0,87
Propyl	$CH_3CH_2CH_2OH$	0,19
Isopropyl	$(CH_3)_2CHOH$	-0,53
Butyl	$CH_3(CH_2)_3OH$	-1,4
Isobutyl	$(CH_3)_2CHCH_2OH$	-3,3

nanographite, than that in bulk regular graphite. Such displacement of the Fermi level in nanographites may be as the result of interaction of surface carbon atoms with some adsorbed molecules. We shall note, that in acceptor graphite intercalation compounds a similar situation are realized and the value of displacement of the Fermi level may be significant (Dresselhaus and Dresselhaus 1981). Obviously, at the validity of the model considered, the position of the Fermi level in nanographites (as well as the sign and the value of charge on graphene layers) may be controlled by adsorption on their surface of different molecules.

We studied the (002) peak displacement at interaction of fibers with several substances and found that the sign and quantity of it, relative the position in a spectrum of initial fibers, depend on the nature of sorbate.

In ACFs with water the (002) peak is located in larger 2θ-angles, than that in a spectrum of macroscopic graphite (Fig. 4). A small narrowing of the (100) peak, determining the identity period along graphene sheets, was also observed. Considered (002) peak displacement and narrowing of the (100) peak are fully reversible. The possible reason for such (002) peak displacement is the large internal pressure from water molecules in pores, as water in the porosity of ACFs has a solid-phase structure with less density than that in the normal conditions (Alcaniz-Monge *et al*. 2002). It is obviously that the decrease of positive charge of graphene layers because of donating of electrons by the adsorbed water molecules may be another reason for this phenomenon. However, we believe, that the reason of discussed (002) X-ray reflection displacement in ACFs with water molecules is their insertion into the space between layers of nanographite. The conduction ESR linewidth of ACFs with water decreases with the temperature. The sign and quantity of (002) peak displacement in ACFs with spirits depends on the nature of spirit (Table 1). This fact also may be explained in the framework of assumption that spirit molecules insert into nanographite intersheet space. In all samples considered the (002) peak displacement is fully

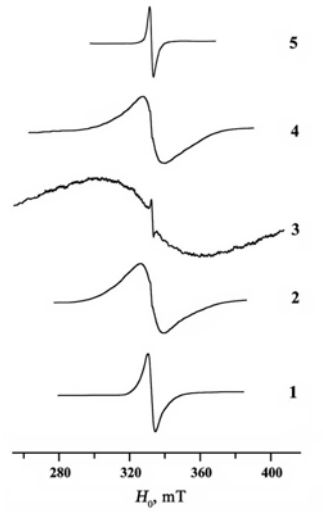

Figure 6. The ESR signal of ACFs vs. amount of Cl_2 dose. 1 – initial spectrum; the amount of Cl_2 dose increases from second to five spectrum.

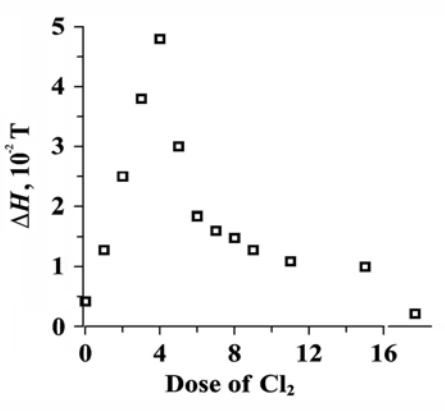

Figure 7. The CESR linewidth of ACFs vs. amount of Cl_2 dose.

reversible. The temperature dependences of conduction ESR linewidth in ACFs with isobutyl and butyl spirits are unusual: it has the clear peak near ≈200 K (Fig. 5).

In ACFs with chlorine the sign and quantity of (002) peak displacement is near for its theoretical value for chlorine molecules in nanographite interlayer space. The conduction ESR linewidth in ACFs with chlorine depends on the amount of chlorine inserted into the part of reactor with a sample (Figs. 6 and 7). For small dose of chlorine the CESR linewidth increases, then form a peak and further decreases with increasing of the chlorine the (002) peak displacement is not fully reversible. The XPS spectrum for carbon of initial fibers is a single asymmetric line with additional excitation signals pi → pi*. After chlorination an additional signal, shifted by ≈1,5÷2 eV with respect to main peak on the binding energy (E_b) scale, arises in the C1s electron spectrum (Fig. 8). The value of E_b for the maximum of Cl2p-electron spectrum is equal to 199.8 ± 0.1 eV, which is close to E_b of the core electrons of chlorine covalently bound with carbon atoms in the series of organic compounds. Chlorination of the ACF does not lead to any significant changes in oxygen spectrum. Only heating the sample in vacuum up to ≈ 150 ÷ 200 ˚C leads to appearance of additional peaks in carbon and oxygen spectra. Observed changes in the C1s electron spectrum and E_b of chlorine core electrons indicate to the covalent binding of chlorine and carbon atoms. Taking into account nearly complete elimination of aliphatic fragments and significant decrease of oxygen content in the sample after preliminary high vacuum evacuation at high temperature, one may conclude that chlorine forms covalent bonds with edge atoms of nanometric graphite particles. Such, for the first time a possibility of chemical modification of graphene edges of nanographite particles with halogen is shown.

Conclusions

An investigation of electronic structure of nanographites - structural blocks of ACFs, has shown that the density of electronic states near the Fermi level of them is more, than that in macroscopic graphite. So, in nanographite, with random distribution of armchair and zigzag edges of graphene sheets, stable localized pi-electronic edge states, generating peak of density of electronic states near the Fermi level, are realized.

In ACFs with different sorbate the sign and quantity of the (002) X-ray diffraction peak shift, relative to its position in a spectrum of initial fibers, depend on the nature of sorbate. For example, among ACFs with spirits, the sign of this shift changes from the negative to the positive at the transferring from propanol- to isopropanol-containing fibers. In the spectrum of ACFs with water, the (002) peak is located in larger 2θ-angles, than that in a spectrum of a macroscopic graphite. In some cases, a small narrowing of the (100) peak, determining the identity period along graphene sheets, was also observed. All above

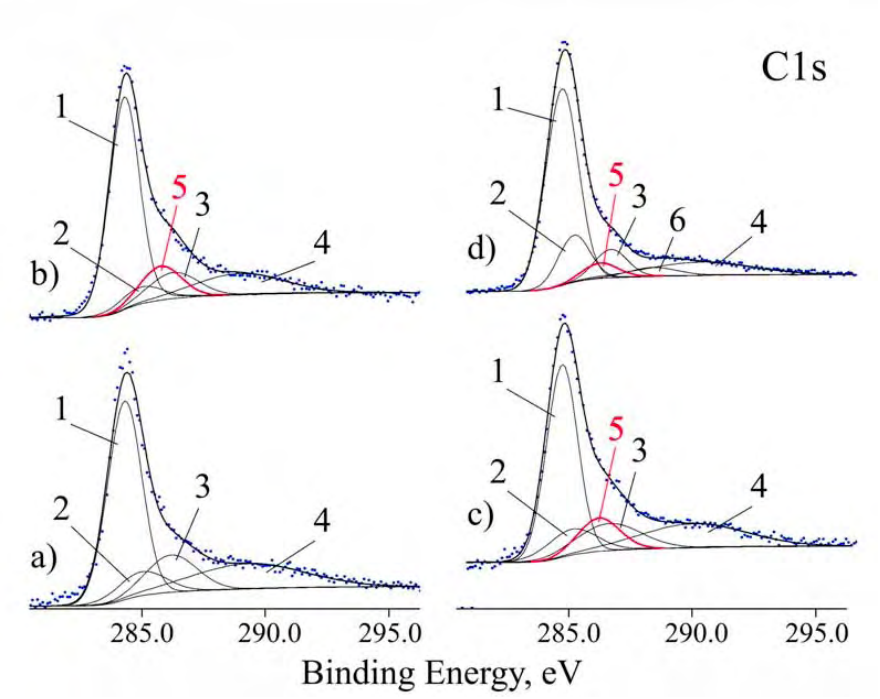

Figure 8. XPS spectrum of ACF after: a) heating in vacuum at $T \approx 800$ ˚C; b) treating with chlorine; c) treating with chlorine after 24 hours in the spectrometer in high vacuum conditions; d) after heating in vacuum at $T \approx 200$ ˚C (1 – nanographite; 2 – aliphatic fragments and/or hydrocarbon contaminations; 3 – C–OH bound; 4 - pi → pi* transition; 5 – C–Cl bound; 6 – C=O bound).

experimental data can be interpreted as a result of nanographite intercalation, at which, simultaneously with increasing of mean distance between graphene sheets, their shift relatively to each other occurs.

This work was supported by the Russian Foundation for Basic Research (grant No. 08-03-00211) and by the Presidium of the Russian AS (The Program of Basic Research on Basic Problems of Physics and Chemistry of Nanosized Systems and Materials).

References

1) Alcaniz-Monge, J., Linares-Solano, A. and Rand, B. (2002). Mechanism of adsorption of water in carbon micropores as revealed by a study of activated carbon fibers. *J. Phys. Chem.*, B106, 3209-3215.
2) Dresselhaus, M.S. and Dresselhaus, G. (1981). Intercalation compounds of graphite. *Adv. Phys.*, 30, 139-326.
3) Dresselhaus, M.S., Dresselhaus, G. and Eklund, P.C. (1996). Science of Fullerenes and Carbon Nanotubes, Academic, San Diego.
4) Fujita, M., Wakabayashi, K., Nakada, K. and Kusakabe, K. (1996). Peculiar localized state at zigzag graphite edge. *J. Phys. Soc. Jpn*., 65, 1920-1923.
5) Harigaya, K. (2001). Mechanism of magnetism in stacked nanographite. *J. Phys.: Condensed Matter*, 13, 1295-1302.
6) Harigaya, K. and Enoki, T. (2002). Mechanism of magnetism in stacked nanographite with open shell electrons. *Chem. Phys. Lett*., 351, 128-134.
7) Klusek, Z., Kozlowski, W., Waqar, Z., Datta, S., Burnell-Gray, J.S., Makarenko, I.V., Gall, N.R.,
8) Rutkov, E.V., Tontegode, A.Ya., Titkov, A.N. (2005). Local electronic edge states of graphene layer deposited on Ir(111) surface studied by STM/CITS. *Appl. Surf. Sci*., 252, 1221-1227.
9) Kobayashi, Y., Fukui, K.-I., Enoki, T., Kusakabe, K., Kaburagi, Y. (2005). Observation of zigzag and armchair edges of graphite using scanning tunneling microscopy and spectroscopy. *Phys. Rev*., B71, 193406 (4).

10) Kaneko, K., Ishii, C., Kanoh, H., Hanzawa, Y., Setoyama, N. and Suzuki, T. (1998). Characterization of porous carbons with high resolution alfa<sub_s>–analysis and low temperature magnetic susceptibility. *Adv. Colloid Interface Sci*., 76-77, 295-320.
11) Marsh H. (2001). Activated carbon compendium, Elsevier Science, Amsterdam.
12) Nakada, K., Fujita, M., Dresselhaus, G. and Dresselhaus, M.S. (1996). Edge state in graphene ribbons: nanometer size effect and edge shape dependence. *Phys. Rev*., B54, 17954-17961.
13) Niimi, Y., Matsui, T., Kambara, H., Tagami, K., Tsukada, M., Fukuyama, H. (2005). Scanning tunneling microscopy and spectroscopy studies of graphite edges. *Appl. Surf. Sci*., 241, 43-48.
14) Shyu, F.L. and Lin, M.F. (2003). Electronic properties of AA-stacked nanographite ribbons. *Physica E*, 16, 214-222.